

La Paz Icefield 02205, 02224, 02226, 02436, 03632, 04841

Unbrecciated basalt

1226.3, 252.5, 244.1, 59.0, 92.6, 56 g



Figure 1: LAP 02205 as found in the LaPaz Icefield. Scale bar at base of counter is in cm.

Introduction

La Paz Icefield (LAP) 02205 (Fig. 1) and its paired masses, LAP 02224, 226, 436, LAP 03632, and LAP 04841 (Fig. 2), are an unbrecciated mare basalt that total ~1930 g. These meteorites were discovered in the LaPaz Icefield in the 2002, 2003, and 2004 ANSMET field seasons and their recovery locations define a linear trend (Fig. 3), which together with their textural, mineralogical, and petrologic similarities argue for pairing. These meteorites represent a unique basaltic

composition not represented in the Apollo collections, and the first unbrecciated mare basaltic meteorite from Antarctica.

Petrography

The LAP meteorites all show similar texture and mineralogy. They are all medium to coarse-grained subophitic basalts, with a dominance of pyroxene, plagioclase and ilmenite (Table 1 and Fig. 4 and 5). Each contains traces of olivine, spinel, troilite, silica, baddeleyite, and

metal. These LAP meteorites also contain heterogeneous melt veins and pockets whose

composition is similar to the bulk composition of the rock with only limited variation.



Figure 2: LAP 02224, 02226, 02436 and 03632 as found in the ice (clockwise from upper left).

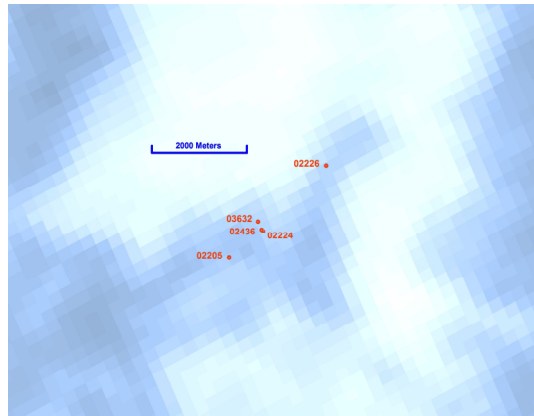


Figure 3: Relative positions of the LAP lunar basaltic meteorites, as discovered in the LaPaz Icefield.

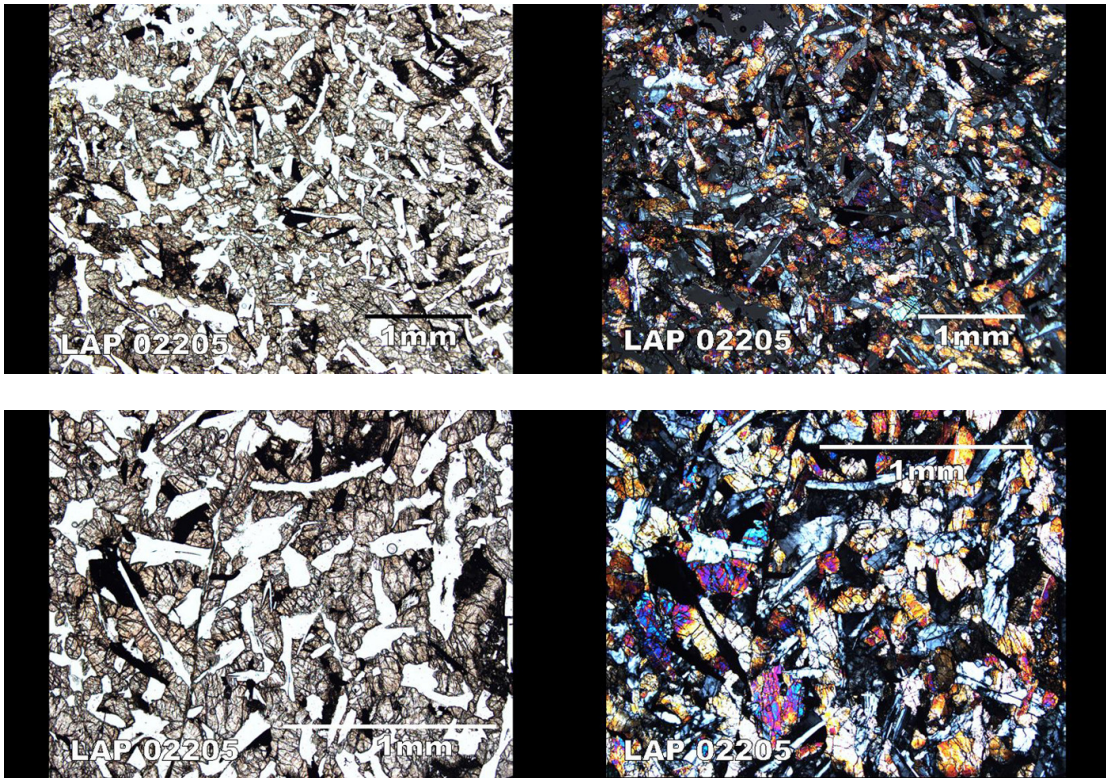


Figure 4: Plane polarized light (left side) and cross nicols (right side) photomicrographs of LAP 02205 illustrating the prevalence of pyroxene (grey) and plagioclase feldspar (white), as well as ilmenite and spinel.

Mineralogy

Several studies have focused on the mineralogy of these basaltic meteorites (Anand et al., 2005; Righter et al., 2005; Zeigler et al., 2005; Day et al., 2006; Joy et al., 2005).

Olivine: Olivines are generally subhedral in shape although some grains have a skeletal habit with subhedral outlines. The olivine compositions range from Fo_{53} to Fo_{62} in the cores to Fo_{46} to Fo_{57} in the rims (Fig. 6). The modal proportion of olivine in four LAP meteorites ranges from 1.1 to 3.6% (Table 1). Righter et al. (2005) proposed that the olivines are out of equilibrium with the bulk rock composition and therefore are xenocrysts.

Pyroxene: The pyroxene is either intersertile or enclosing plagioclase within all of the rocks. Pyroxene grains have strong chemical variation from pigeonite to ferroaugite (Fig. 7). The ferroaugite has strong Fe enrichment and Mg depletion towards the rims of grains and they contain pigeonite cores. Thin augite lamellae are also present within some grains indicative of slow cooling rates. This feature results from subsolidus exsolution of pigeonite into orthopyroxene and augite. LAP basalt pyroxenes also exhibit clear affinity with lunar Fe/Mn ratios (Fig. 8).

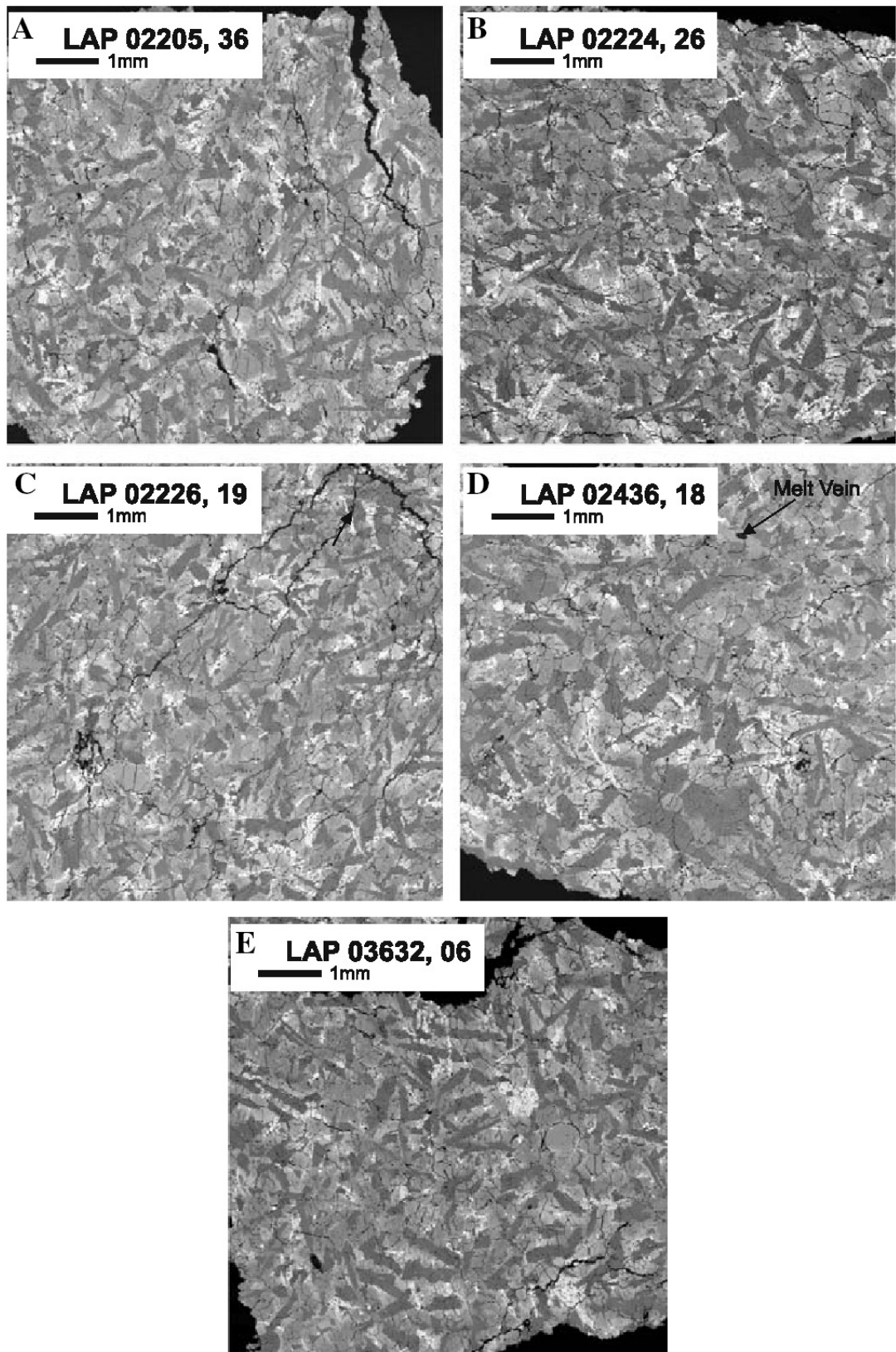


Figure 5: Back scattered electron images of five of the La Paz lunar basaltic meteorites, illustrating the textures within these paired samples (from Day et al., 2006).

Table 1: Modal analysis of the LAP meteorites

| | LAP 02205 | LAP 02226 | LAP 02224 | LAP 02436 | LAP 03632 | LAP 02205 | LAP 02205 | LAP 02226 | LAP 02224 | LAP 02436 |
|----------------|--------------|--------------|--------------|--------------|--------------|--------------|--------------|--------------|--------------|--------------|
| reference | 1 | 1 | 1 | 1 | 1 | 2 | 3 | 3 | 3 | 3 |
| Pyroxene | 43.9 | 51.2 | 52.9 | 53.1 | 50.7 | 56.9 | 51.5 | 50.5 | 46.9 | 46.6 |
| Plagioclase | 45.3 | 36.3 | 39.2 | 34.7 | 39.1 | 33.1 | 31.9 | 32.1 | 32.3 | 34.6 |
| Ilmenite | 3.7 | 5.1 | 3.8 | 4.6 | 3.1 | 3.3 | 3.48 | 3.91 | 3.86 | 3.99 |
| Olivine | 1.1 | 1.7 | 1.6 | 1.5 | 2.7 | 1.2 | 2.33 | 2.71 | 3.63 | 3.20 |
| Spinel | 1.5 | 1.0 | 0.7 | 0.8 | 0.2 | 0.4 | 0.34 | 0.45 | 0.40 | 0.39 |
| Phosphate | 0.7 | 1.4 | 0.8 | 1.7 | 0.7 | 0.3 | 2.14 | 2.09 | 1.78 | 2.00 |
| Troilite | 1.4 | 0.6 | 0.3 | 1.3 | 1.1 | 0.2 | 0.25 | 0.24 | 0.24 | 0.22 |
| Fayalite symp. | 2.5 | 2.8 | 0.7 | 2.3 | 2.4 | 1.5 | 3.09 | 2.90 | 3.58 | 4.83 |
| Other# | tr | tr | tr | tr | tr | tr | 0.10 | 0.20 | 2.20 | - |

#Fe metal, melt veins, and baddeleyite are present in trace amounts in all samples.

References: 1) Righter et al. (2005), 2) Anand et al. (2005), 3) Ziegler et al. (2005).

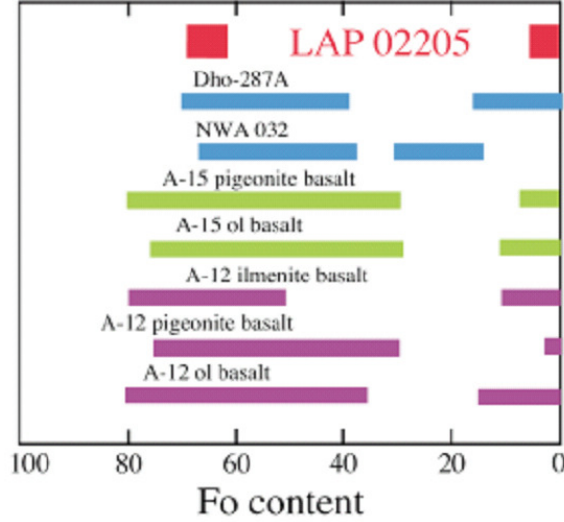


Figure 6: Olivine composition in LAP 02205 compared to Dho-287A, NWA032, and other Apollo mare basalt samples.

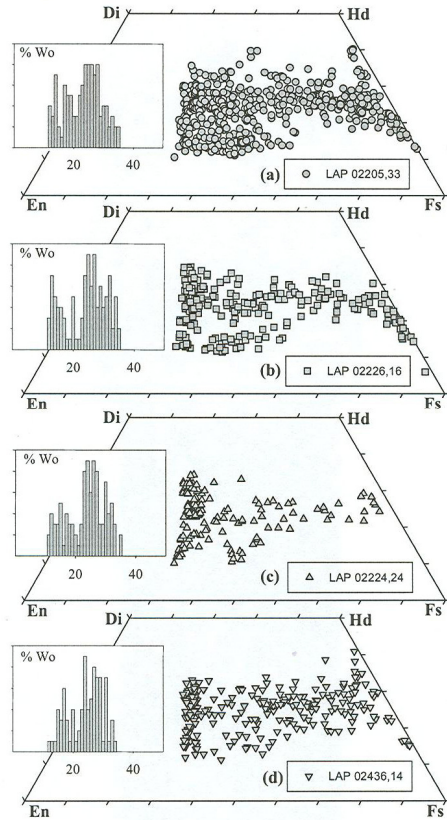


Figure 7: Pyroxene quadrilateral diagrams showing the range of pyroxene from pigeonite and augite cores to more Fe-rich rims (from Ziegler et al., 2005).

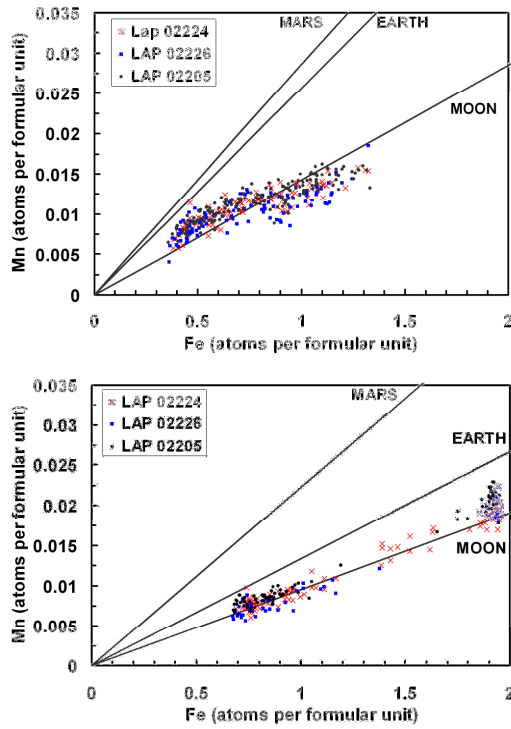


Figure 8: Fe/Mn ratios for pyroxenes for LAP 02205, 02224 and 02226 (from Joy *et al.*, 2005).

Plagioclase: Plagioclase is a dominant component in the LAP meteorites and ranges from 32 to 45 modal percent (Table 1). It occurs commonly as laths but in some cases has a blocky texture. The plagioclase compositions of the LAP meteorites range from An₈₅ to An₈₉.

Ilmenite: Ilmenite occurs within the LAP meteorites as the most dominant opaque. The ilmenites co-precipitated with pyroxene and plagioclase from the cooling magma as lath-like crystals. Modal percent of ilmenite within these meteorites ranges from 3.1% to 5.1% (Table 1). Ilmenite in these samples contain very low concentrations of MgO with a range from 0.02 to 0.24 wt. %.

Baddeleyite: Occurs in association with ulvöspinel, ilmenite and troilite, and is typically 20 to 40 μm in size.

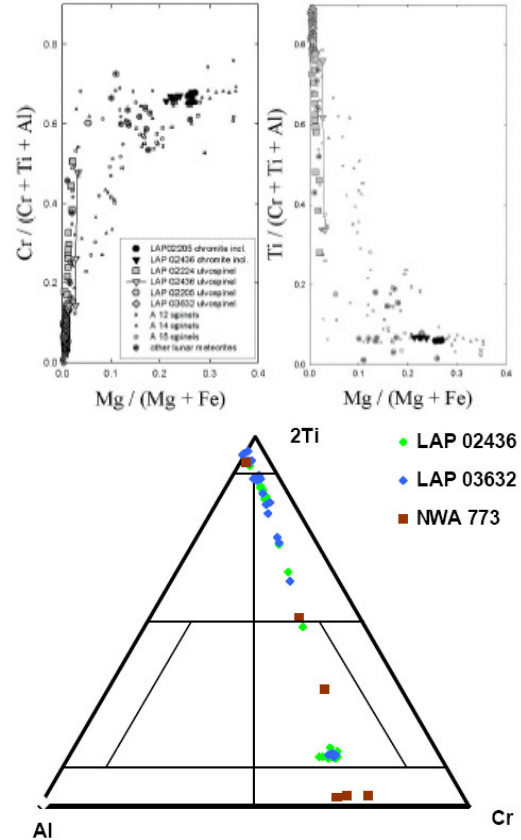


Figure 9a: Range of spinel compositions in LAP meteorites with Cr-rich spinel found as inclusions in olivine, followed by later Cr ulvöspinel that co-crystallizes with ilmenite (from Righter *et al.*, 2005). Figure 9b: Transition of Cr-rich to Ti-rich spinels in NWA 773 and LAP basalt series of samples (from Hallis *et al.*, 2007).

Spinel: Spinel in these samples make up 0.2 to 1.5 modal % (Table 1). Ulvöspinel occurs as equant grains with little zonation. Small chromite inclusions are present within olivine phenocrysts and are thought to have been the earliest spinels to crystallize. Chromite crystallization was followed by Cr – poor ulvöspinel (Fig. 9).

Metal: Metal grains are small (10-20 μm) and are commonly associated with spinel and sulphide within the LAP meteorites. There is a large amount of compositional variation within the metal grains throughout these rocks (Day *et al.*,

2005, 2006), but it is thought to be indigenous to the sample, rather than affected by meteoritic contamination (Fig. 10).

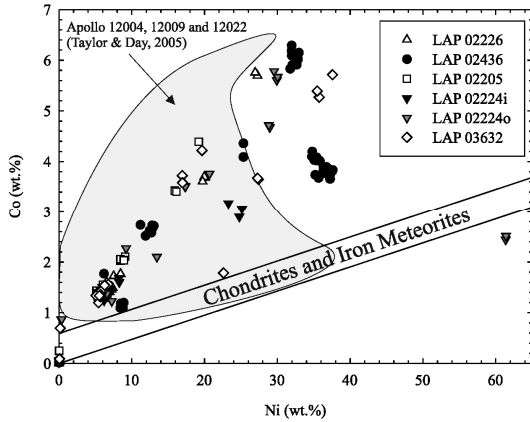


Figure 10: Ni vs. Co (all in wt%) for metal grains in the LaPaz basalt suite. The extensive variation is indigenous to the sample rather than contributed by meteoritic contamination (Day et al., 2006).

Troilite: Troilite is present in trace amounts and with equant morphology. Troilite is typically found in association with oxide grains and in some cases with metal.

Silica: The LAP meteorites contain cristobalite found as trace amounts, and usually associated with late stage mesostasis or symplectitic fayalite, plagioclase and metal (Fig. 11).

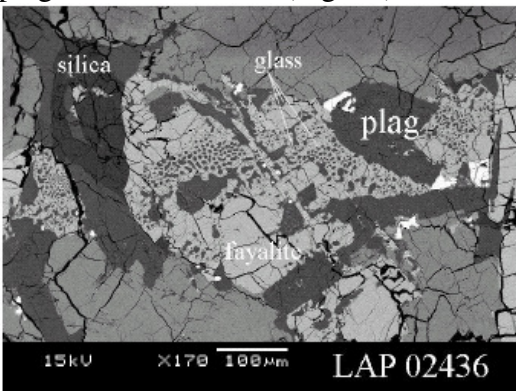


Figure 11: Symplectitic texture in the mesostasis of LAP 02436, involving fayalite and glass (from Righter et al., 2005).

Melt veins: Ubiquitous melt veins are heterogeneous in composition and commonly contain areas with relict mineral grains.

Textural studies of the La Paz lunar basaltic meteorites indicate cooling rates (based on plagioclase, pyroxene and ilmenite) of 0.1 to 0.3 C/hr, consistent with an origin near the middle of a slowly cooled lava flow (Day and Taylor, 2007). These cooling rates are in general agreement, but slightly lower than those inferred by Koizumi et al. (2005) based on experimental studies.

Chemistry

Several groups have reported INAA and ICP-MS analyses of relatively small (35 to 50 mg) chips of LAP 02205 and its paired samples (Table 2).

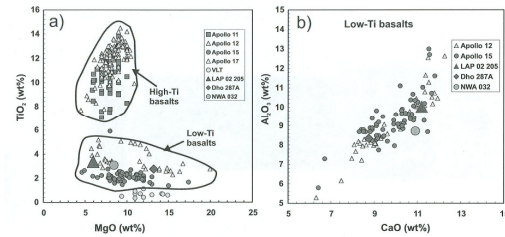


Figure 12: LAP basalts fall within the low Ti basalt field with respect to TiO_2 , MgO , CaO and Al_2O_3 (from Zeigler et al., 2005).

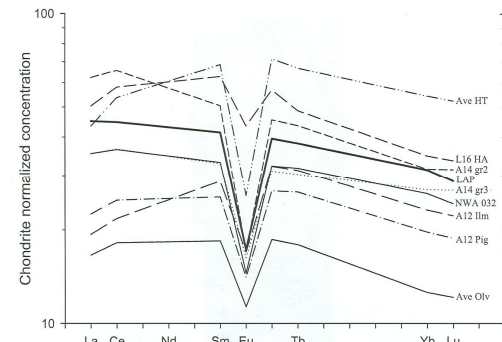


Figure 13: Rare earth element diagram for LAP 02205 compared to many other Apollo basalts and NWA032 (from Zeigler et al., 2005).

TiO_2 compositions are similar to low Ti basalts such as Apollo 12 ilmenite and olivine basalts (Fig. 12). They also show relatively high Al_2O_3 and seem to be depleted in MgO compared to the other lunar samples. Europium

anomalies are similar to other mare basalts, except that the absolute REE contents are high, suggesting a more evolved or fractionated basalt compared to many Apollo mare basalts (Fig. 13).

Table 2a. Chemical composition of LAP 02205

| reference | 1 | 2 | 2 | 2 | 2 | 2 | 2 | 2 | 3 | 4 | 5 |
|--------------------------------|-------|-------|-------|-------|-------|-------|-------|-------|-------|---------------------|--------|
| weight | - | 35.3 | 40.2 | 40.2 | 34.5 | 41.3 | 48.9 | avg | 50 | melt vein avg | |
| split | | ,20-1 | ,20-2 | ,20-3 | ,24-1 | ,24-2 | ,24-3 | | | | ,21 |
| technique | b | d,e | b | | d,e |
| SiO ₂ % | 44.5 | 45 | 45.3 | 45.2 | 45.3 | 44.6 | 45.2 | 45.1 | 45.2 | 44.08 | 46.0 |
| TiO ₂ | 3.43 | 3.34 | 3.33 | 3.34 | 2.99 | 3.28 | 3.13 | 3.23 | 3.38 | 4.18 | 3.11 |
| Al ₂ O ₃ | 10.13 | 9.84 | 10.18 | 10.48 | 9.63 | 8.98 | 10.2 | 9.9 | 10 | 14.52 | 9.95 |
| Cr ₂ O ₃ | | 0.26 | 0.22 | 0.26 | 0.33 | 0.32 | 0.33 | 0.29 | 0.19 | 0.16 | 0.29 |
| FeO | 21.69 | 22.9 | 22.8 | 21.9 | 21.7 | 23.3 | 21.6 | 22.3 | 23.2 | 18 | 21.8 |
| MnO | 0.28 | 0.28 | 0.3 | 0.29 | 0.28 | 0.34 | 0.32 | 0.3 | 0.23 | 0.22 | 0.32 |
| MgO | 5.58 | 5.87 | 5.46 | 5.69 | 7.17 | 7.11 | 6.68 | 6.34 | 5.99 | 5.41 | 6.32 |
| CaO | 11.23 | 11.1 | 11.2 | 11.4 | 11.1 | 10.5 | 11.3 | 11.1 | 11.2 | 11.56 | 11.4 |
| Na ₂ O | 0.42 | 0.39 | 0.42 | 0.41 | 0.38 | 0.36 | 0.39 | 0.39 | 0.33 | 0.56 | 0.39 |
| K ₂ O | | 0.08 | 0.09 | 0.07 | 0.06 | 0.07 | 0.06 | 0.07 | 0.11 | 0.13 | 0.10 |
| P ₂ O ₅ | 0.12 | 0.11 | 0.11 | 0.1 | 0.09 | 0.08 | 0.08 | 0.09 | 0.12 | 0.17 | 0.17 |
| S % | | | | | | | | | | | 0.16 |
| sum | 97.38 | 99.17 | 99.41 | 99.14 | 99.03 | 98.94 | 99.29 | 99.11 | 99.95 | 98.99 | 100.00 |
| Sc ppm | | 59 | 58 | 57.8 | 59.5 | 58.9 | 60.4 | 59 | 58.6 | | 52.8 |
| V | | | | | | | | | 129 | | 92 |
| Cr | 1751 | 1511 | 1767 | 2290 | 2180 | 2230 | 1962 | | | | 1625 |
| Co | 34.6 | 33.9 | 34 | 37.8 | 40.4 | 37 | 36.3 | 37.3 | | | 35.4 |
| Ni | 0 | 50 | 30 | 50 | 30 | 30 | 32 | 27.6 | | | 42.4 |
| Cu | | | | | | | | | | | 18.6 |
| Zn | | | | | | | | | | | 27.5 |
| Ga | | | | | | | | | | | 3.74 |
| Ge | | | | | | | | | | | |
| As | | | | | | | | | | | |
| Se | | | | | | | | | | | |
| Rb | | | | | | | | | 2.1 | | 1.67 |
| Sr | 150 | 160 | 190 | 130 | 130 | 110 | 144 | 135.3 | | | 109 |
| Y | | | | | | | | 73.2 | | | 57.0 |
| Zr | 200 | 260 | 250 | 210 | 150 | 140 | 199 | 200.3 | | | 172 |
| Nb | | | | | | | | 14.7 | | | 11.9 |
| Mo | | | | | | | | | | | |
| Ru | | | | | | | | | 3.6 | | |
| Rh | | | | | | | | | 1.2 | | |
| Pd ppb | | | | | | | | | 8.3 | | |

| | | | | | | | | | |
|--------|------|------|------|------|------|------|------|-------|------|
| Ag ppb | | | | | | | | | |
| Cd ppb | | | | | | | | | |
| In ppb | | | | | | | | | |
| Sn ppb | | | | | | | | | |
| Sb ppb | | | | | | | | | |
| Te ppb | | | | | | | | | |
| Cs ppm | | | | | | | | 0.1 | 0.03 |
| Ba | 166 | 154 | 150 | 124 | 134 | 152 | 147 | 164.7 | 122 |
| La | 14.7 | 15.3 | 14.2 | 11.6 | 15.3 | 14.6 | 14.4 | 13.4 | 9.97 |
| Ce | 38.3 | 39.6 | 36.6 | 32.2 | 37 | 36 | 36.7 | 37.31 | 26.3 |
| Pr | | | | | | | | 5.15 | 4.04 |
| Nd | 25 | 28 | 23 | 20 | 27 | 20 | 24 | 25.12 | 19.1 |
| Sm | 8.6 | 8.89 | 8.35 | 7.04 | 8.51 | 8.19 | 8.28 | 7.56 | 6.05 |
| Eu | 1.36 | 1.41 | 1.36 | 1.2 | 1.26 | 1.29 | 1.31 | 1.24 | 0.98 |
| Gd | | | | | | | | 9.95 | 7.81 |
| Tb | 1.89 | 2.02 | 1.91 | 1.63 | 1.95 | 1.86 | 1.88 | 1.93 | 1.44 |
| Dy | | | | | | | | 12.08 | 9.35 |
| Ho | | | | | | | | 2.45 | 2.00 |
| Er | | | | | | | | 6.71 | 5.40 |
| Tm | | | | | | | | 0.94 | 0.84 |
| Yb | 7.3 | 7.4 | 7 | 6.1 | 7 | 6.7 | 6.9 | 6.37 | 5.30 |
| Lu | 0.99 | 1.03 | 0.96 | 0.83 | 0.95 | 0.94 | 0.95 | 0.88 | 0.82 |
| Hf | 6.27 | 6.42 | 6.06 | 5.1 | 5.71 | 5.5 | 5.84 | 5.39 | 4.50 |
| Ta | 0.8 | 0.8 | 0.79 | 0.69 | 0.67 | 0.69 | 0.74 | 0.77 | 0.60 |
| W ppb | | | | | | | | 0.2 | |
| Re ppb | | | | | | | | | |
| Os ppb | | | | | | | | | |
| Ir ppb | | | | | | | | 1.8 | |
| Pt ppb | | | | | | | | 31.5 | |
| Au ppb | | | | | | | | | |
| Th ppm | 2.24 | 2.34 | 2.2 | 1.79 | 2.01 | 1.93 | 2.08 | 2.33 | 1.79 |
| U ppm | 0.61 | 0.52 | 0.67 | 0.55 | 0.53 | 0.42 | 0.54 | 0.55 | 0.45 |

technique (a) ICP-AES, (b) ICP-MS, (c) IDMS, (d) fused bead EMPA, (e) INAA, (f) RNAA, (g) SSM

References: 1) Joy et al. (2005); 2) Zeigler et al. (2005); 3) Anand et al. (2005); 4) Righter et al. (2005); 5) Day et al. (2006).

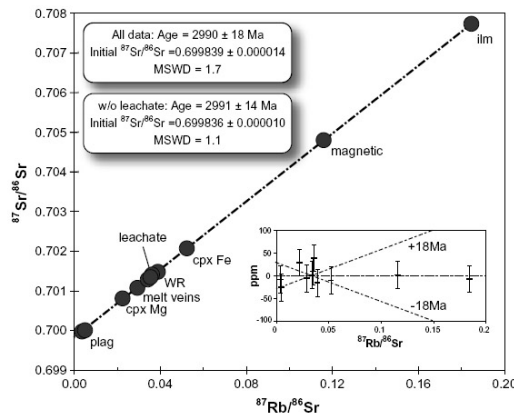


Figure 14: Rb-Sr whole rock and mineral separate isochron for LAP 02205 (from Rankenburg et al., 2007).

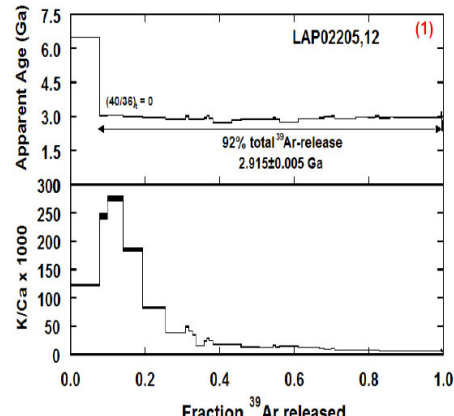


Figure 15: Ar plateau age and K/Ca ratio for LAP 02205 (Fernandes and Burgess, 2006).

Table 2b. Light and/or volatile elements for LAP 02205

| Anand05 | |
|---------|------|
| Li ppm | 11.7 |
| Be | 1.37 |
| C | |
| S | |
| F ppm | |
| Cl | |
| Br | |
| I | |
| Pb ppm | 1 |
| Hg ppb | |
| Tl | |
| Bi | |

Platinum group element analyses of the LAP basalts (Day et al., 2006) have been used to argue for the addition of late chondritic material to the mantle of the Moon after a giant impact and lunar core formation. Although this simple approach is based on comparisons between lunar and terrestrial basalt PGE systematics, it does not apparently assess or take into account differences in sulfide saturation between lunar and terrestrial basalts. Nonetheless these high quality and low concentration PGE data for the lunar basalts provides useful constraints of the origin of the Moon.

Radiogenic age dating

Several groups have reported radiometric age determinations of the LAP basalts. A whole rock Rb-Sr isochron based on mineral separates from LAP 02205 yields an age of 2.990 (± 0.018) Ga (Fig. 14; Rankenburg et al., 2007) which is identical within error to the age obtained by Shih et al. (2005) of 3.02 (± 0.03) Ga. Ar dating of LAP 02205 whole rock material yields an age of 2.936 Ga. The latter age is nearly identical to that obtained using UV laser Ar dating of LAP 02205 samples yields

an age of 2.915 Ga (Fig. 15; Fernandes and Burgess, 2006). Whole rock Sm-Nd dating of LAP 02205 has resulted in an age of 2.992 (± 0.025) Ga (Rankenburg et al., 2007). And a U-Pb age based on several in situ analyses of phosphates yields an age of 2.929 Ga (Fig. 17; Anand et al., 2005, 2006). This is clearly a young mare basalt.

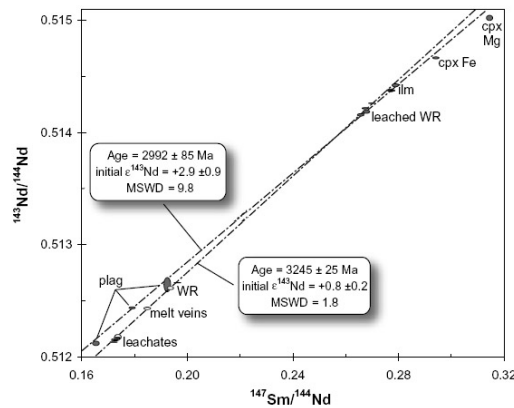


Figure 16: Sm-Nd whole rock and mineral separate isochron for LAP 02205 (from Rankenburg et al., 2007).

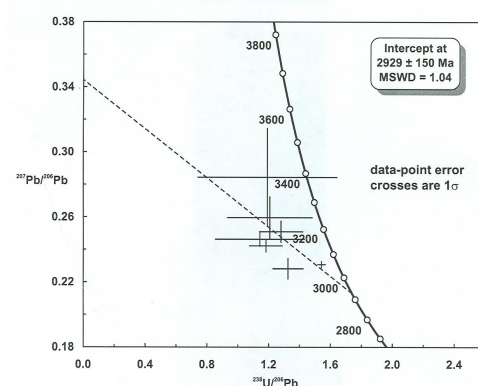


Figure 17: A 3D linear regression of apatite U/Pb measurements for the lunar meteorite LAP 02205 (Anand et al., 2005, 2006).

Cosmogenic isotopes and exposure ages

Measurements of ^{10}Be , ^{26}Al , ^{36}Cl , and ^{41}Ca indicate that the LaPaz basalts were ejected from the Moon 55 (± 5) Ka ago, and fell to Antarctica 20 (± 5) Ka

ago (Nishiizumi et al., 2006). Together with compositional and textural links, these ages are consistent with launch pairing of the NWA 032 (and paired

samples) and LAP 02205 (and paired samples) lunar basalts.

Table 3: Chemical composition of stones paired with LAP 02205

| | | | | | | | | | | | | | |
|--------|------|------|------|------|------|------|------|------|------|------|------|------|------|
| Sn ppb | | | | | | | | | | | | | |
| Sb ppb | | | | | | | | | | | | | |
| Te ppb | | | | | | | | | | | | | |
| Cs ppm | | | | | | | | | | | | | |
| Ba | 153 | 163 | 144 | 144 | 157 | 142 | 139 | 86 | 126 | 157 | 163 | 128 | 163 |
| La | 12.5 | 14.5 | 11.4 | 11.8 | 12.7 | 12.4 | 11.0 | 10.6 | 11.8 | 13.6 | 12.7 | 11.7 | 13.2 |
| Ce | 33.6 | 38.8 | 30.8 | 32.9 | 34.5 | 34.4 | 31.9 | 27.3 | 31.6 | 36.9 | 33.8 | 32.1 | 36.2 |
| Pr | | | | | | | | | | | | | |
| Nd | 22 | 25 | 16 | 18 | 26 | 24 | 18 | 20 | 19 | 22 | 21 | 26 | 23 |
| Sm | 7.48 | 8.61 | 6.84 | 7.24 | 7.62 | 7.42 | 6.80 | 6.32 | 7.05 | 8.13 | 7.58 | 7.15 | 7.91 |
| Eu | 1.21 | 1.30 | 1.12 | 1.19 | 1.25 | 1.22 | 1.20 | 1.02 | 1.14 | 1.28 | 1.20 | 1.20 | 1.27 |
| Gd | | | | | | | | | | | | | |
| Tb | 1.73 | 2.03 | 1.66 | 1.68 | 1.77 | 1.73 | 1.67 | 1.51 | 1.65 | 1.85 | 1.76 | 1.65 | 1.83 |
| Dy | | | | | | | | | | | | | |
| Ho | | | | | | | | | | | | | |
| Er | | | | | | | | | | | | | |
| Tm | | | | | | | | | | | | | |
| Yb | 6.5 | 7.3 | 6.0 | 6.2 | 6.6 | 6.4 | 5.9 | 5.3 | 6.1 | 7.0 | 6.5 | 6.3 | 6.8 |
| Lu | 0.91 | 1.00 | 0.82 | 0.87 | 0.91 | 0.90 | 0.84 | 0.73 | 0.86 | 1.00 | 0.91 | 0.89 | 0.95 |
| Hf | 5.67 | 6.33 | 5.04 | 5.25 | 5.65 | 5.49 | 5.01 | 4.18 | 5.19 | 5.97 | 5.59 | 5.18 | 5.85 |
| Ta | 0.74 | 0.80 | 0.61 | 0.70 | 0.73 | 0.75 | 0.63 | 0.57 | 0.63 | 0.76 | 0.76 | 0.67 | 0.69 |
| W ppb | | | | | | | | | | | | | |
| Re ppb | | | | | | | | | | | | | |
| Os ppb | | | | | | | | | | | | | |
| Ir ppb | | | | | | | | | | | | | |
| Pt ppb | | | | | | | | | | | | | |
| Au ppb | | | | | | | | | | | | | |
| Th ppm | 2.13 | 2.39 | 1.80 | 1.87 | 2.11 | 2.04 | 1.91 | 1.42 | 2.00 | 2.34 | 1.96 | 1.96 | 2.17 |
| U ppm | 0.48 | 0.64 | 0.44 | 0.51 | 0.54 | 0.43 | 0.44 | 0.37 | 0.56 | 0.57 | 0.42 | 0.55 | 0.59 |

technique (a) ICP-AES, (b) ICP-MS, (c) IDMS, (d) Ar, (e) INAA, (f) RNAA, (g) SSMS, (h) fused bead EMPA

Table 3: Chemical composition of stones paired with LAP 02205 (continued)

| <i>reference</i> | 5 | 5 | 5 | 5 | 5 | 2 | 5 |
|--------------------------------|-------|-------|-------|-------|-------|------|------|
| <i>sample</i> | 02224 | 02224 | 02226 | 02436 | 03632 | LAP | LAP |
| <i>weight</i> | 27.9 | 27.3 | 28.8 | 28.3 | 27.7 | 641 | ? |
| <i>split</i> | 17 | 18 | 13 | 20 | 8 | avg | avg |
| <i>technique</i> | d,e | d,e | d,e | d,e | d,e | d,e | d,e |
| SiO ₂ % | 45.9 | 45.3 | 45.3 | 45.3 | 45.7 | 45.3 | 45.6 |
| TiO ₂ | 2.94 | 3.27 | 3.20 | 3.23 | 3.26 | 3.11 | 3.17 |
| | | | 10.0 | | | | |
| Al ₂ O ₃ | 9.45 | 9.95 | 7 | 9.52 | 9.65 | 9.79 | 9.76 |
| Cr ₂ O ₃ | 0.32 | 0.30 | 0.31 | 0.36 | 0.33 | 0.31 | 0.32 |
| FeO | 22.1 | 22.0 | 22.0 | 22.1 | 21.7 | 22.2 | 21.9 |
| MnO | 0.31 | 0.29 | 0.30 | 0.30 | 0.31 | 0.29 | 0.31 |
| MgO | 7.19 | 6.84 | 6.84 | 7.71 | 7.25 | 6.63 | 7.02 |
| | | | | | 11.0 | | |
| CaO | 11.1 | 11.3 | 11.2 | 10.8 | 11.2 | 9 | 11.2 |
| Na ₂ O | 0.35 | 0.38 | 0.35 | 0.33 | 0.33 | 0.38 | 0.36 |
| K ₂ O | 0.10 | 0.11 | 0.10 | 0.08 | 0.08 | 0.07 | 0.10 |
| P ₂ O ₅ | 0.17 | 0.16 | 0.16 | 0.13 | 0.12 | 0.10 | 0.15 |
| SO ₃ | 0.16 | 0.14 | 0.15 | 0.15 | 0.17 | | 0.15 |
| | | | | | | 99.2 | |
| <i>sum</i> | 100 | 100 | 100 | 100 | 100 | 8 | 100 |
| Sc ppm | 59.2 | 57.3 | 58.8 | 54.0 | 58.4 | 59.2 | |
| V | 114 | 109 | 110 | 110 | 113 | | |
| Cr | 2368 | 2172 | 2192 | 2298 | 2300 | 2096 | |
| Co | 37.6 | 36.9 | 36.9 | 37.5 | 37.9 | 37.0 | |
| Ni | 20.6 | 18.5 | 21.9 | 26.0 | 21.8 | | |
| Cu | 19.8 | 19.4 | 18.6 | 16.4 | 19.8 | | |
| Zn | 30.8 | 29.6 | 27.1 | 26.3 | 30.2 | | |
| Ga | 4.29 | 4.07 | 4.18 | 3.58 | 4.28 | | |
| Ge | | | | | | | |
| As | | | | | | | |
| Se | | | | | | | |
| Rb | 1.86 | 1.74 | 1.82 | 1.50 | 1.79 | | |
| Sr | 124 | 122 | 122 | 104 | 124 | 133 | |
| Y | 64.9 | 64.9 | 64.0 | 55.1 | 64.5 | | |
| Zr | 194 | 190 | 185 | 161 | 189 | 183 | |
| Nb | 13.3 | 12.9 | 12.8 | 11.1 | 13.2 | | |
| Mo | | | | | | | |
| Ru | | | | | | | |
| Rh | | | | | | | |
| Pd ppb | | | | | | | |
| Ag ppb | | | | | | | |
| Cd ppb | | | | | | | |
| In ppb | | | | | | | |
| Sn ppb | | | | | | | |
| Sb ppb | | | | | | | |
| Te ppb | | | | | | | |
| Cs ppm | 0.04 | 0.04 | 0.04 | 0.02 | 0.02 | | |

| | | | | | | |
|--------|------|------|------|------|------|------|
| Ba | 137 | 131 | 134 | 112 | 134 | 145 |
| La | 11.4 | 11.5 | 11.5 | 10.2 | 11.5 | 13.1 |
| Ce | 29.6 | 29.3 | 30.6 | 25.3 | 29.8 | 34.7 |
| Pr | 4.57 | 4.5 | 4.67 | 3.93 | 4.61 | |
| Nd | 21.5 | 21.5 | 21.9 | 18.6 | 21.6 | 22 |
| Sm | 6.75 | 6.73 | 6.79 | 5.84 | 6.87 | 7.74 |
| Eu | 1.10 | 1.07 | 1.11 | 0.93 | 1.13 | 1.24 |
| Gd | 9.08 | 8.73 | 8.92 | 7.57 | 9.04 | |
| Tb | 1.64 | 1.62 | 1.65 | 1.41 | 1.64 | 1.79 |
| Dy | 10.6 | 10.4 | 10.6 | 9.1 | 10.6 | |
| Ho | 2.30 | 2.21 | 2.28 | 1.94 | 2.28 | |
| Er | 6.09 | 6.04 | 6.08 | 5.26 | 6.10 | |
| Tm | 0.95 | 0.94 | 0.95 | 0.82 | 0.96 | |
| Yb | 5.95 | 5.91 | 5.92 | 5.12 | 5.97 | 6.59 |
| Lu | 0.93 | 0.90 | 0.91 | 0.79 | 0.92 | 0.92 |
| Hf | 5.02 | 4.92 | 4.90 | 4.25 | 5.00 | 5.58 |
| Ta | 0.68 | 0.65 | 0.65 | 0.57 | 0.67 | 0.71 |
| W ppb | | | | | | |
| Re ppb | | | | | | |
| Os ppb | | | | | | |
| Ir ppb | | | | | | |
| Pt ppb | | | | | | |
| Au ppb | | | | | | |
| Th ppm | 2.04 | 2.04 | 2.06 | 1.72 | 2.03 | 2.04 |
| U ppm | 0.49 | 0.50 | 0.50 | 0.43 | 0.49 | 0.52 |

Processing

LAP 02205 was initially processed in the summer of 2003, generating splits ,1 ,2 ,3 and ,4 (Figs. 18, 19, 20). Later allocations in the Fall of 2003 resulted in extensive subdivision of ,2 (Fig. 21 and Table 4).

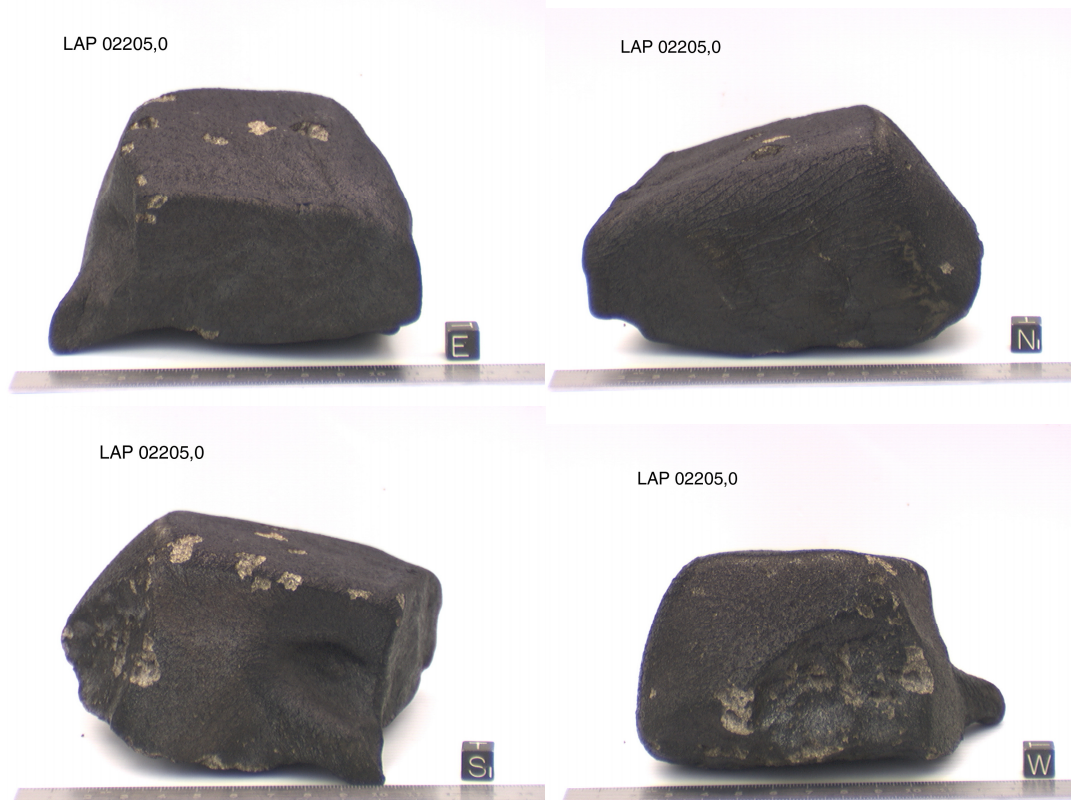


Figure 18: Four laboratory views of LAP 02205 with 1 cm orientation cube for scale.

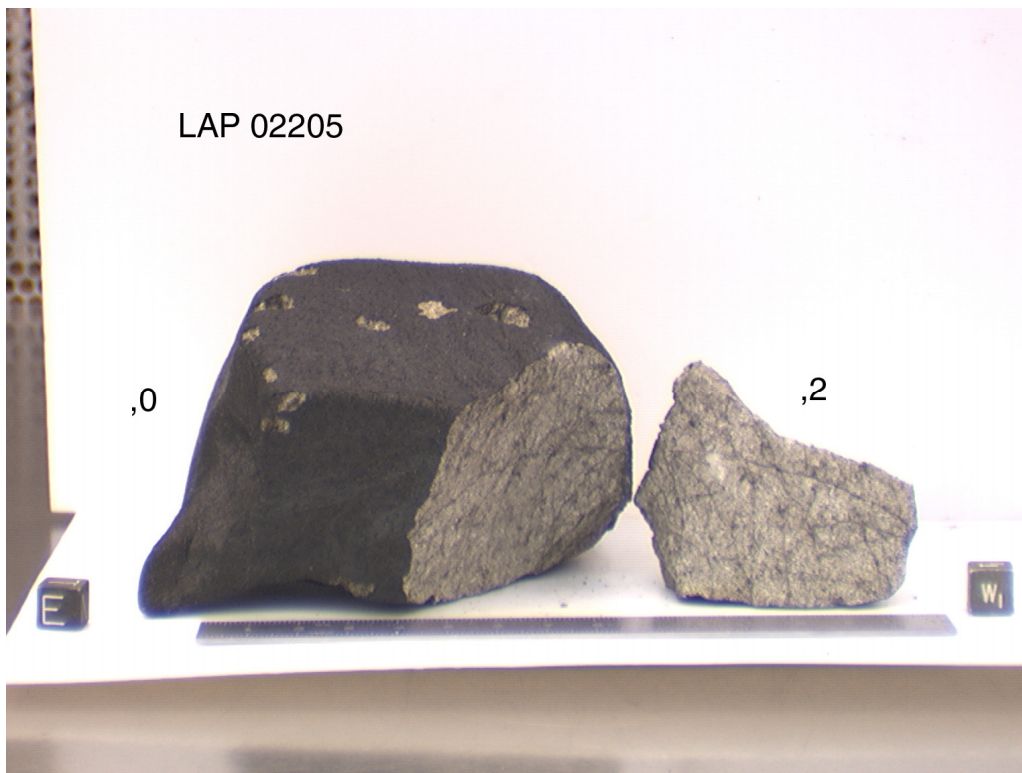


Figure 19: Initial processing of LAP 02205, showing splits ,0 and ,2. Cubes are 1 cm.

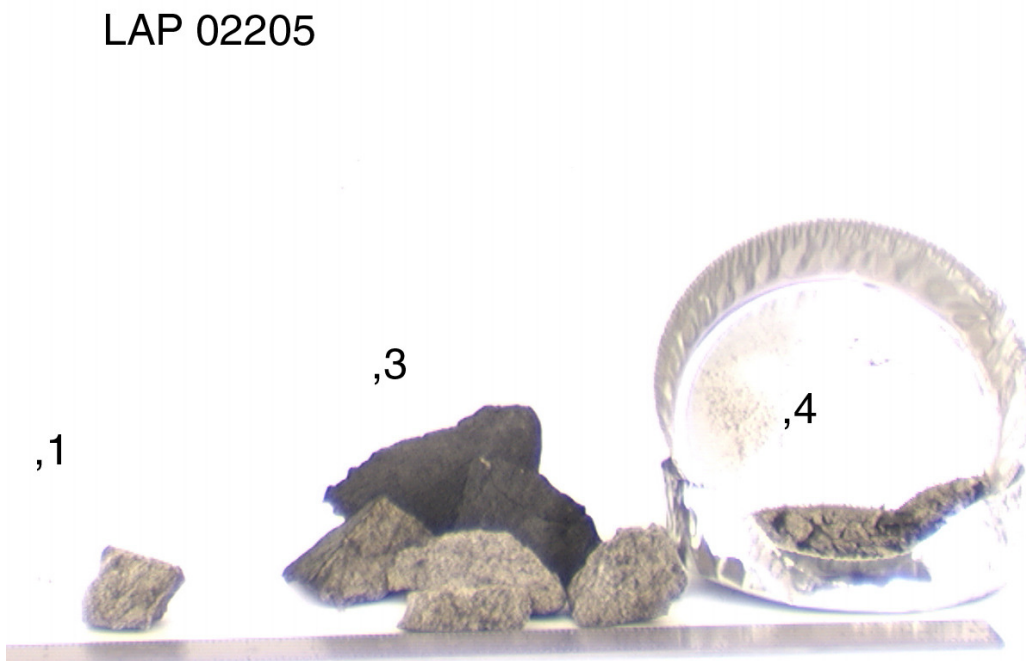
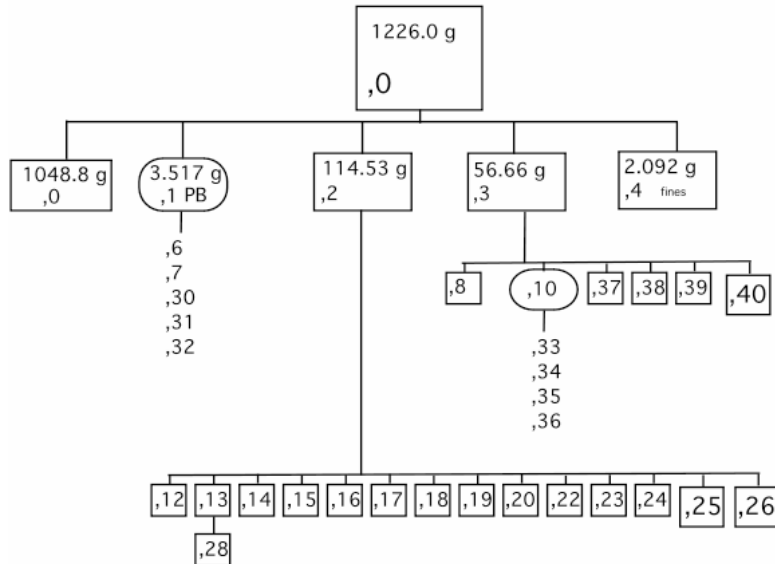


Figure 20: LAP 02205, 1 ,3 and ,4. Most allocations have been derived from these splits 1, 2 and 3 (see Table 3).

LAP 02205



reconstructed in September 2004, from
information in datapacks, by K. Righter

Figure 21: Genealogy of LAP 02205 based on information available in datapacks at JSC.

Table 4: Split allocations of LAP 02205 (7/04)

| Split | parent | Mass (g) | PI or location | comment |
|-------|--------|----------|----------------|---------------|
| 0 | - | 1048 | JSC | As of 9/04 |
| 1 | 0 | 3.467 | Potted butt | Potted butt |
| 2 | 0 | 97.044 | JSC | Documented pc |
| 3 | 0 | 49.358 | JSC | chips |
| 6 | 1 | 0.010 | McCoy/SI | Thin section |
| 7 | 1 | 0.010 | JSC | Thin section |
| 8 | 3 | 0.107 | R.N. Clayton | Int. chip |
| 12 | 2 | 0.016 | Bizarro | Int. chip |
| 13 | 2 | 0.209 | JSC | Int. chip |
| 14 | 2 | 0.345 | Nyquist | Int. chip |
| 15 | 2 | 0.652 | Nishizumi | Ext. chip |
| 16 | 2 | 0.484 | Mikouchi | Int. chip |
| 17 | 2 | 0.535 | Nishizumi | Int. chip |
| 18 | 2 | 0.318 | Brandon | Int. chip |
| 19 | 2 | 1.572 | L.A. Taylor | Int. chip |
| 20 | 2 | 0.258 | Korotev | Int. chip |
| 22 | 2 | 0.403 | Nishizumi | Ext. chip |
| 23 | 2 | 4.660 | Brandon | Int. chip |
| 24 | 2 | 0.265 | Korotev | Int. chip |
| 28 | 13 | 0.099 | Arai | Int. chip |
| 30 | 1 | 0.010 | Brandon | Thin section |

| | | | | |
|----|----|-------|-------------|--------------|
| 31 | 1 | 0.010 | L.A. Taylor | Thin section |
| 32 | 1 | 0.010 | S. Russell | Thin section |
| 33 | 10 | 0.010 | Korotev | Thin section |
| 34 | 10 | 0.010 | Mikouchi | Thin section |
| 35 | 10 | 0.010 | Arai | Thin section |
| 36 | 10 | 0.010 | L.A.Taylor | Thin section |
| 37 | 3 | 0.334 | Busemann | Int chip |
| 38 | 3 | 0.150 | Herzog | Int chip |
| 39 | 3 | 0.172 | Herzog | Int chip |

Lunar Meteorite Compendium by K Righter 2008